Journal of Chromatography A, 1530 (2017) 129–137

Contents lists available at ScienceDirect

Journal of Chromatography A

journal homepage: www.elsevier.com/locate/chroma

Full length article

Mechanical characterisation of agarose-based chromatography resins for biopharmaceutical manufacture

Mauryn C. Nweke [a], R. Graham McCartney [b], Daniel G. Bracewell [a,*]

[a] Department of Biochemical Engineering, University College London, Bernard Katz Building, Gower Street, London, WC1E 6BT, United Kingdom
[b] Eli Lilly & Co. Dunderrow, Kinsale, Co. Cork, Ireland

ARTICLE INFO

Article history:
Received 21 July 2017
Received in revised form
15 November 2017
Accepted 16 November 2017
Available online 20 November 2017

Keywords:
Mechanical characterisation
Chromatography media
Agarose beads
Pressure-flow
Dynamic mechanical analysis

ABSTRACT

Mechanical characterisation of agarose-based resins is an important factor in ensuring robust chromatographic performance in the manufacture of biopharmaceuticals. Pressure-flow profiles are most commonly used to characterise these properties. There are a number of drawbacks with this method, including the potential need for several re-packs to achieve the desired packing quality, the impact of wall effects on experimental set up and the quantities of chromatography media and buffers required. To address these issues, we have developed a dynamic mechanical analysis (DMA) technique that characterises the mechanical properties of resins based on the viscoelasticity of a 1 ml sample of slurry. This technique was conducted on seven resins with varying degrees of mechanical robustness and the results were compared to pressure-flow test results on the same resins. Results show a strong correlation between the two techniques. The most mechanically robust resin (Capto Q) had a critical velocity 3.3 times higher than the weakest (Sepharose CL-4B), whilst the DMA technique showed Capto Q to have a slurry deformation rate 8.3 times lower than Sepharose CL-4B. To ascertain whether polymer structure is indicative of mechanical strength, scanning electron microscopy images were also used to study the structural properties of each resin. Results indicate that DMA can be used as a small volume, complementary technique for the mechanical characterisation of chromatography media.

© 2017 The Author(s). Published by Elsevier B.V. This is an open access article under the CC BY license (http://creativecommons.org/licenses/by/4.0/).

1. Introduction

Manufacturers must ensure that chromatography media meet a broad range of requirements before use for the separation/purification of biological products. These requirements include a number of safety considerations (leachables, toxicology), performance (capacity, specificity, throughput), cost (capital investment, longevity) and stability, among others [1]. Stability can be split broadly into two categories – chemical and mechanical. The chemical resistance of chromatography media is dependent on the coupling chemistry as well as the choice of spacer and ligand chemistry and stability. Whereas, the mechanical stability is dependent largely on the choice and composition of the base material, particle size distribution, particle porosity, and to a lesser extent, ligand and ligand deployment [2,3].

The base material is chosen based on a number of factors such as cost, the properties of the material to be processed and surface area and mass transfer characteristics, giving rise to parameters such as dynamic binding capacity (DBC) maximum flow rates, maximum number of cycles etc. Based on this, different manufacturers use different composite materials for their chromatographic media [4]. Agarose is a commonly used base matrix material in biopharmaceutical purification as it relatively straightforward to manufacture and customise certain properties such as porosity and specific binding properties. This paper focuses particularly on MabSelect™, Sepharose ™ and Capto™ media (GE Healthcare, Uppsala, Sweden).

Agarose is one of two main constituents of agar and is generally extracted from seaweed. It is composed of a polysaccharide polymer material formed of repeating units of 1–3-linked β-D galactose and 1,4-linked 3,6-anhydro-α-L-galactose [5]. Once the agar has been processed, the agarose is in the form of a dry powder. It is then dissolved in an aqueous solution >85° C, causing the chains to degrade [3,6]. When the solution reaches a certain viscosity, it is cooled and poured, whilst simultaneously being stirred into a non-polar organic solvent which contains an emulsifier. These conditions induce the formation of spherical beads (emulsification). The stirring and cooling rates are a key parameters in determining certain structural characteristics such as porosity, pore size distri-

* Corresponding author.
E-mail address: d.bracewell@ucl.ac.uk (D.G. Bracewell).

https://doi.org/10.1016/j.chroma.2017.11.038
0021-9673/© 2017 The Author(s). Published by Elsevier B.V. This is an open access article under the CC BY license (http://creativecommons.org/licenses/by/4.0/).

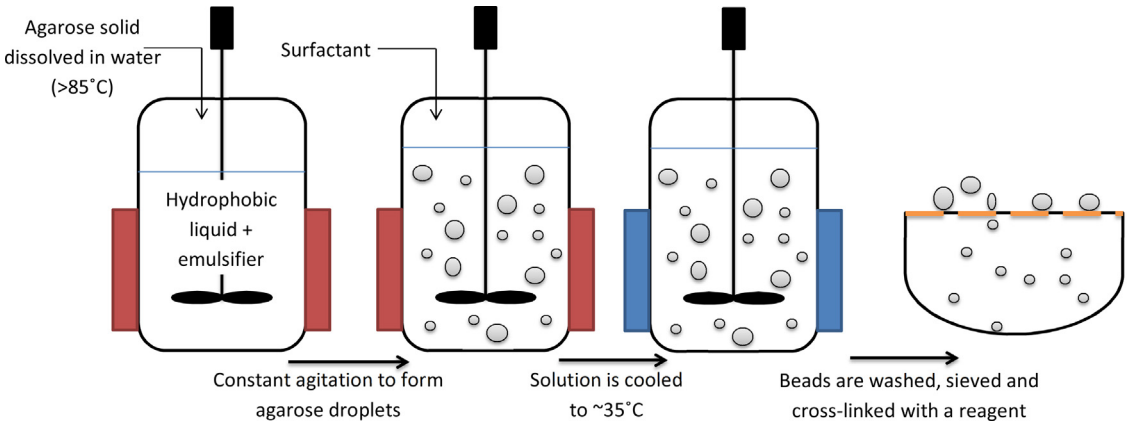

Fig. 1. General method for making porous agarose beads. The agarose solid is dissolved in water heated to about 90° C. This is then added to a stirred vessel containing a hydrophobic solution (eg. Toluene or mineral oil) together with an emulsifier. The solutions are immiscible meaning that constant agitation causes the formation of agarose droplets. A surfactant is added to prevent droplet coalescing. The solution is then cooled to below the gelation point of agarose (~35° C) and the beads are then washed, sieved to narrow the size distribution and cross-linked with a reagent.

bution and particle size distribution, which tends to range from 20 to 300 μm [4] (Fig. 1).

Upon formation, the beads are insoluble and sediment into the higher density water phase, as opposed to the organic solvent phase. The beads are subsequently cross-linked with a reagent such as epichlorohydrin. The extent to which this is done is one of the critical factors that determine the rigidity of the matrix. However, caution must be taken at this step as over-cross-linking may reduce porosity, ligand deployment and compressibility characteristics [7,8]. When the process is completed, the resin can be used in various applications such as size exclusion and desalting. It may alternatively go on to be functionalised with different ligand chemistries, after which it can be used in a number of modes for various biopharmaceutical applications [1,3,9–11].

To ensure consistency in the structural and mechanical properties of chromatography media, the media has to be well characterised. Structural integrity testing involves looking at pore size and particle size distributions and porosity, which can generally be ascertained indirectly by observing titration curves or static capacity. There have also been reports on developing lab-based procedures that involve the use of micromanipulation [9,12]. A better idea of mechanical and column performance is usually determined by pressure-flow characterisation. This technique involves gradually increasing the flow rate and observing a rise in the pressure profile in the column. At a certain flow velocity, the pressure in the column will continue to rise without further increase to the flow rate. It is at this point that the critical velocity has been reached and the column has 'failed' [13].

The advantages of this method include the ability to determine the behaviour of chromatography media in a packed bed and how mechanical properties vary with media viscosity, pH, ionic strength etc. However, a drawback of this method is that it requires that the operator adheres to stringent packing criteria to obtain meaningful data. When packing columns, several re-packs may be required to achieve the desired asymmetry and each resin, depending on its chemical and mechanical properties, has its own specific packing criteria. Furthermore, it is necessary to use a column of a suitable diameter, such that wall effects that support the resin in narrow columns do not dominate [14]. The bed height also needs to be representative, as pressure drop directly correlates to the height of the bed, meaning heights of 15 cm or greater are typically used [15]. For these reasons, the pressure-flow technique consumes large quantities of chromatographic media and buffers, which is costly [16].

To address these drawbacks, we have developed the use of dynamic mechanical analysis (DMA) (Fig. 2). This technique

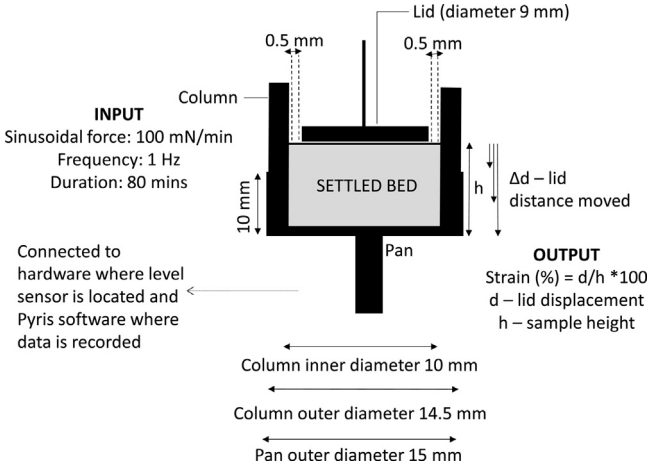

Fig. 2. Schematic of DMA set up and dimensions (not drawn to scale). The lid has a diameter of 10 mm and the column that sits inside the pan has an inner diameter of 11 mm and an outer diameter of 14 mm. A sinusoidal force of 100mN is applied at a frequency of 1 Hz over a period of 80 min. The output is strain v time, where strain is the displacement of the lid relative to the sample height.

involves applying a small deformation to a sample in a cyclic manner and allows for the sample material to respond to changes in stress, temperature, strain, frequency, force as well as other parameters. It is used widely in the bioengineering sector and the field of biosciences to characterise the viscoelastic properties of various biological tissue and other biomaterials. Traditionally, the stress and strain parameters are used to calculate Young's modulus to give an indication of changes in elastic properties. Moroni et al., 2006 [17] used the technique to investigate the use of scaffolds to mimic human tissue. They found that the technique was particularly sensitive to pore size changes in scaffolds. With increasing porosity in the scaffolds, there was a decrease in elastic properties, which corresponded to an increase in strain. It has also been used to look at the mechanical properties of materials similar to agarose gels, such as hydrogels. Meyvis & Stubbe 2002 [18] used DMA as a comparative technique to shear rheometry to investigate mechanical properties of pharmaceutical hydrogels. They found a strong correlation between the two techniques but observed that DMA can be used to investigate many more mechanical parameters than solely viscoelasticity.

We have applied the use of DMA to investigate the viscoelastic properties of small quantities of seven agarose-based

Table 1
Packing flowrates for Sepharose 4FF, Sepharose 6FF, Q-Sepharose HP, MabSelect and Capto Q.

Resin	Packing flow rates
Sepharose 4 FF, Sepharose 6 FF, Q Sepharose HP	400 cm/hr – 2 min
MabSelect	500 cm/hr – 2 min
Capto Q	600 cm/hr – 2 min

resins, namely: Sepharose CL–4 B (SCL4B), Sepharose 4FF (S4FF), Sepharose CL–6 B (SCL6B), Sepharose 6FF (S6FF), Q-Sepharose High Performance (Q-HP), MabSelect™ (MabSelect) and Capto™ Q (Capto Q) (GE Healthcare, Uppsala, Sweden). We investigate how the slurries respond to strain over a fixed period of time. We then look to draw correlations between the results obtained from pressure-flow and DMA experiments to ascertain whether DMA can be used as complementary technique for the mechanical characterisation of chromatography media.

2. Materials and methods

2.1. Pressure-flow

2.1.1. Equipment

A bench-scale column with adjustable column length and inner diameter of 1.6 cm (model XK16, GE Healthcare, Uppsala, Sweden) was used. This was operated on the AKTA Pure (GE Healthcare, Uppsala, Sweden). Column pressure drop (ΔP) was measured using the internal pressure measurement devices installed in the feed delivery system of the AKTA Pure and the volumetric flow rate was measured manually using the method employed by [15].

2.1.2. Chromatography media

Sepharose CL-4B, Sepharose CL-6B, Sepharose 4 Fast Flow, Sepharose 6 Fast Flow, Q Sepharose High Performance, MabSelect and Capto Q (GE Healthcare, Uppsala, Sweden) were used in this study. These agarose-based chromatography resins have an average particle size of 80 μm, with a bead size distribution of between 24 and 165 μm. The mechanical differences between the seven resins lie in the agarose content and the extent of structural cross-linking present.

MabSelect and Capto Q are made of highly cross-linked agarose, whereas Sepharose CL-4B/CL-6B, Sepharose 4 FF/6 FF and Q Sepharose HP are structurally simpler in terms of their cross-linking. However Sepharose 6 FF, CL-6B, Q Sepharose HP and MabSelect all contain the same percentage of agarose in their matrices (6%), while Sepharose CL–4 B and Sepharose 4 FF contain 4% and Capto Q 7%.

2.1.3. Procedure

Packing – All chromatography media was made up to 50% slurry concentration. The same procedure was repeated for all seven resins. 30 ml of slurry was poured into the column and allowed to gravity settle overnight. The adaptor was lowered into the supernatant to start the flow pack. All columns were packed at 15 cm/hr for 60 min and subsequently at 30 cm/hr for 30 min. The columns shown in Table 1 were further consolidated. The top adaptor was then lowered to the top of the bed. The packing medium used for all buffers was distilled H_2O (dH_2O).

Performance testing – 2% v/v of acetone was measured and added into 30 ml of dH_2O in a 50 ml falcon tube (CELLSTAR®, UK). 1 ml of this solution was injected into a 600 μl loop and then loaded onto the column. The eluent used in this study was dH_2O at 30 cm/hr. A peak was then generated within 30 min. The asymmetry was calculated using the in-built function on the Unicorn 6.4 software.

Pressure-flow method – The flow rate of the packing buffer was continually gradually increased until a 35 kPa increase in pressure drop was observed, as described by Tran et al., 2007 [15]. At this point, the flow rate and any changes in bed height were manually recorded. At a certain flow rate, the pressure began to increase exponentially with no further change to the flow velocity. At this point it was deemed that the critical velocity for the column had been reached.

2.2. Dynamic mechanical analysis

2.2.1. Column/holder design

10 identical cylindrical blocks of transparent acrylic were drilled with an inner diameter of 11 mm, an outer diameter of 14 mm and a height of 15 mm. The bottom was wrapped in a thin sheet of parafilm (0.1 mm thickness) to contain the slurry.

2.2.2. Sample preparation

An aliquot of 10 ml of each resin was placed into a labelled 50 ml falcon tube and centrifuged for 5 min at 3000 rpm (Eppendorf centrifuge 5810 R, Thermo Fisher Scientific, UK) and the slurry concentration was noted based on the volume ratio of liquid to slurry in the falcon tube. The storage buffer (20% ethanol) was decanted, replaced with their respective packing buffers and the slurry solution was made up to a 70% slurry concentration. The aliquots were resuspended and the procedure was repeated until the storage buffer had been completely removed. 1.42 ml of each aliquot was pipetted into their respectively labelled holder and left to settle overnight, such that their settled bed height was 1 cm. A consistent slurry concentration is important in achieving a uniform settled bed volume and height for comparable strain measurements across all resins.

2.2.3. DMA procedure

DMA was carried out on the DMA 7e hardware, with a TAC 7/DX controller and Pyris Manager software (PerkinElmer, UK). In this procedure the force reading is zeroed, the weight of the probe is tared and the probe position is zeroed when the lid is lowered to the base of the pan. The lid is lifted and the holder containing the slurry is placed onto the pan. The lid is lowered to the top of the resin bed, the height is read and the methodology is started. In this methodology, the lid applies a force of 100mN/min at a frequency of 1 Hz for 80 min and a time-strain plot is generated simultaneously. Upon completion of the methodology, the slope of the line is manually fitted from the origin to the point before ultimate compression (Fig. 6) using the in-built slope function in the Pyris Manager software.

2.3. Scanning electron microscopy

All samples were critical point dried and imaged using the same protocol described in Nweke et al., 2016 [19].

3. Results & discussion

The resins used in this study were selected based on their differences in percentage of agarose content and differences observed in their fibrous structure, pore size distribution and cross-linking via scanning electron microscopy (Fig. 5, Table 2). Their mechanical properties are characterised using the standard pressure-flow method and this will then be compared to results from dynamic mechanical analysis.

3.1. Pressure-flow

In this technique, the flow rate is manually increased until a runaway rise in the pressure profile is observed. The flow rate at

Table 2
Nominal bead size, pore size, % agarose and extent of cross linking of the resins used in this study. Information is based on GE Healthcare data sheets unless cited otherwise.

Resin	Bead size range (μm)	Pore size range (nm)	% agarose	Extent of cross-linking
Sepharose CL-4B	45–165	~42-70 [28,26]	4%	Simple
Sepharose CL-6B	45–165	~24-70 [28,26]	6%	Simple
Sepharose 4 Fast Flow	~90	~45-100 [28,26]	4%	Simple
Sepharose 6 Fast Flow	~90	~29-70 [28,26]	6%	Simple
Q-Sepharose High Performance	24–44	~70 [26]	6%	Simple
MabSelect	~85	~60 –130 [29,26]	6%	High
Capto Q	~90	~50 [26]	7%	High

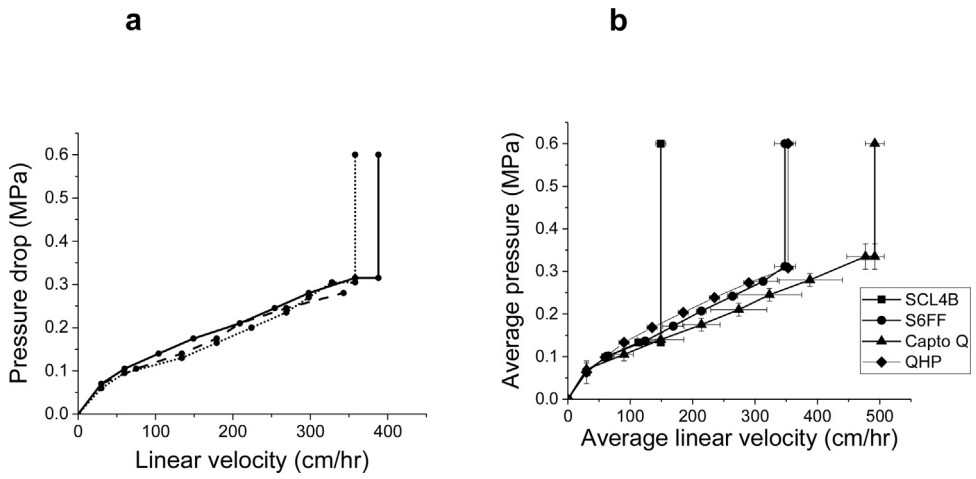

Fig. 3. (a) Pressure-flow plot showing 3 repeats for Sepharose 6FF (6% cross-linked agarose) (one solid line, one dashed line, one dotted line) (circles). (b) Pressure-flow plot showing averages of 3 out of the 7 resins – Sepharose CL–4 B (4% cross-linked agarose) (squares), Sepharose 6FF (6% cross-linked agarose) (circles) and Capto Q (7% highly cross-linked agarose) (triangles). Error bars representing pressure and flow rate are +/− one standard deviation taken from the 3 repeats.

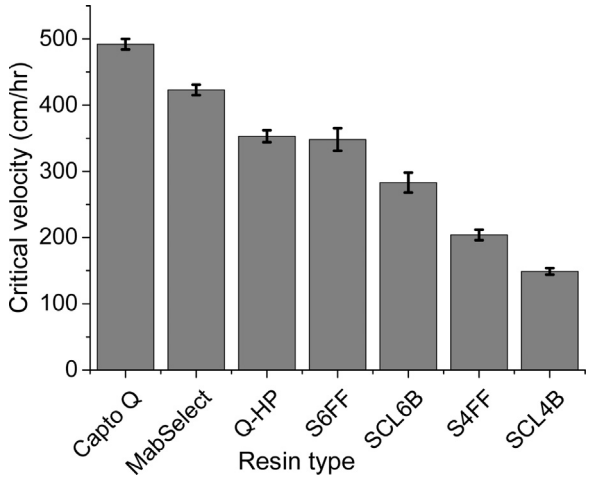

Fig. 4. Critical velocity for each resin obtained using the pressure-flow technique in an XK16 column, bed height 15 cm. Each bar represents an average of the point before column failure. The error bars represent the standard deviation of 3 repeats of each resin. Capto Q (7% highly cross-linked agarose), MabSelect (6% highly cross-linked agarose), Q Sepharose HP (6% cross-linked agarose), Sepharose 6FF (6% cross-linked agarose), Sepharose CL–6 B (6% cross-linked agarose), Sepharose 4FF (4% cross-linked agarose), Sepharose CL–4 B (4% cross-linked agarose).

which this occurs is converted to linear velocity. This is the point at which the column has 'failed' and is termed the critical velocity. The more rigid the resin is, the higher the critical velocity. Three repeats of the procedure (section 2.1) were conducted for all seven resins and the averages are plotted. The standard deviations from the average (based on the repeats) are represented by the error bars (Fig. 3). The degree to which any individual repeat may vary is reliant mainly on column packing and the resulting asymmetry. The probability that a column will pack in exactly the same way, despite using the same procedure is low. This is represented by the asymmetry value obtained. Although the asymmetry differed for all repeats, it was maintained in the range of 0.8-1.2 (which may have required multiple repacks to achieve). A reduction in bed height during the changes to flow velocity may also be observed [15].

Fig. 4 shows the critical velocities for each resin using the pressure-flow characterisation technique using an XK16 column with a bed height of 15 cm. Capto Q has the highest critical velocity at 492 cm/hr, followed by MabSelect – 423 cm/hr, Q-Sepharose HP – 353 cm/hr, Sepharose 6FF – 348 cm/hr, Sepharose CL–6 B – 283 cm/hr, Sepharose 4FF – 204 cm/hr and Sepharose CL–4 B – 149 cm/hr.

The results show that Capto Q is the least compressible of the 7 resins, followed by MabSelect. This is expected as both resins are made of highly cross-linked agarose polymers and contain 7% and 6% agarose respectively. Q-HP and S6FF are cross-linked resins that contain 6% agarose. These two resins have quasi-identical critical velocities. Their main structural differences are observed in their average bead size and their average pore size distributions (Fig. 5, Table 2) so their dynamic behaviour in the column is not exactly the same (Fig. 3b – Q-HP exhibits slightly higher pressure drop). S6FF resins are 2–3 times larger in size (d_p) compared to Q-HP, however the average pore size of S6FF (and Fast Flow resins in general) is approximately 2–3 times smaller than that of Q-HP [20–22]. It has been established that both pore size distribution and bead size contribute to the mechanical properties of chromatography media [23,9]. The trade-off between these two parameters, as well as their identical mechanical traits, may explain why both resins have very similar critical velocity values.

The results also show the differences in mechanical strength between SCL6 B and S6FF, as well as SCL4 B and S4FF. Both pairs of resins are cross-linked and contain 6% and 4% agarose in their matrices respectively, however both fast flow resins are mechanically

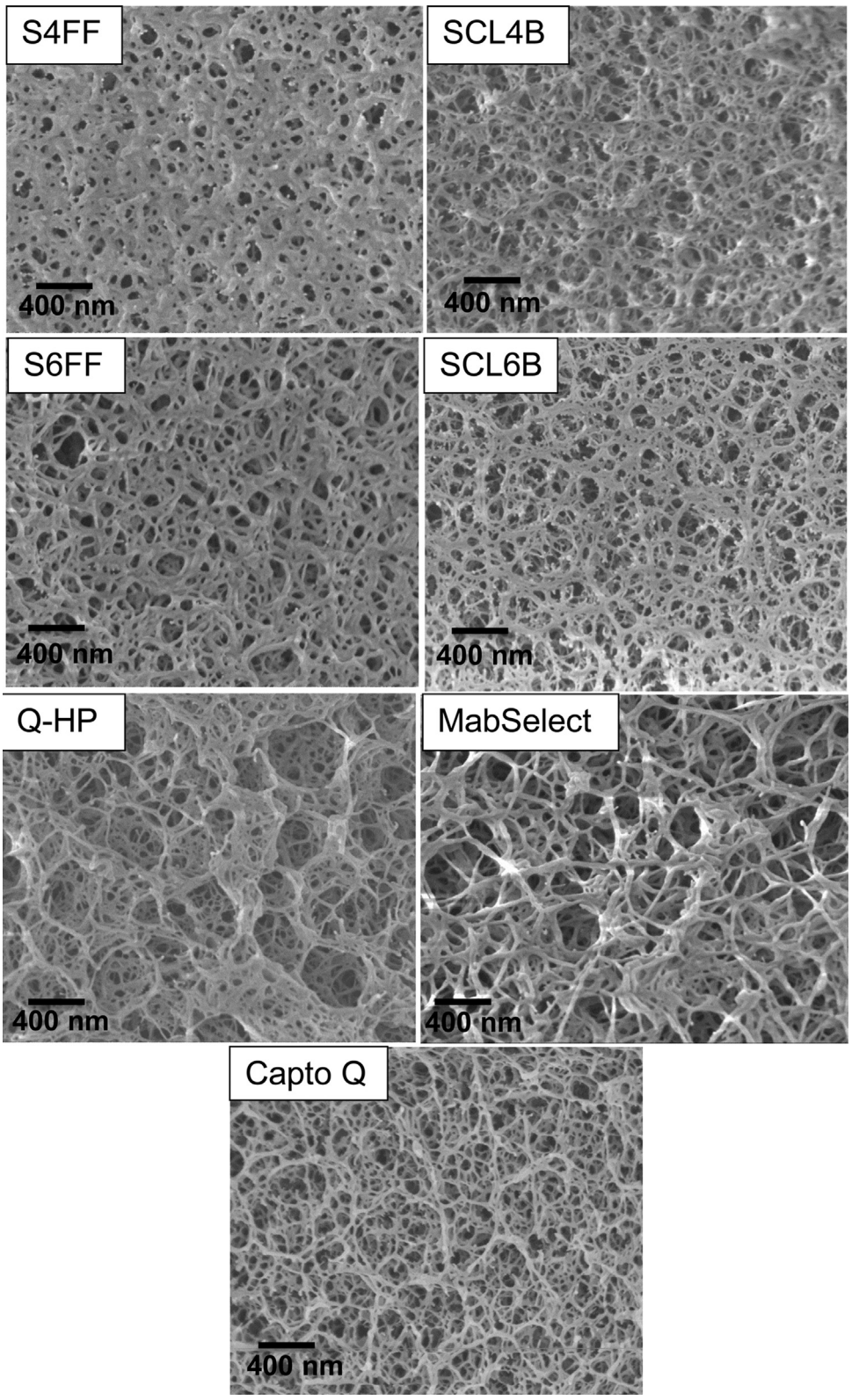

Fig. 5. Scanning electron micrographs showing: Sepharose 4FF (4% cross-linked agarose), Sepharose CL–4 B (4% cross-linked agarose), Sepharose 6FF (6% cross-linked agarose), Sepharose CL–6 B (6% cross-linked agarose), Q-Sepharose HP (6% cross-linked agarose), MabSelect (6% highly cross-linked agarose) and Capto Q (7% highly cross-linked agarose). All images are taken post-critical point drying. Each image is x40000 magnification, 2.0 kV. Scale: 1 cm bar represents 400 nm of resin in all micrographs.

stronger than their – CL counterparts. In both cases, the fast flow resins withstand much higher flow rates according to the manufacturer's specification, which may indicate that their cross-linking was more extensive. Scanning electron micrographs were obtained to show the structural properties of each resin, which were used to ascertain whether polymer structure is indicative of mechanical strength. Their micrographs show that they are structurally different (Fig. 5). SCL6B, for example, appears to be more fibrous and

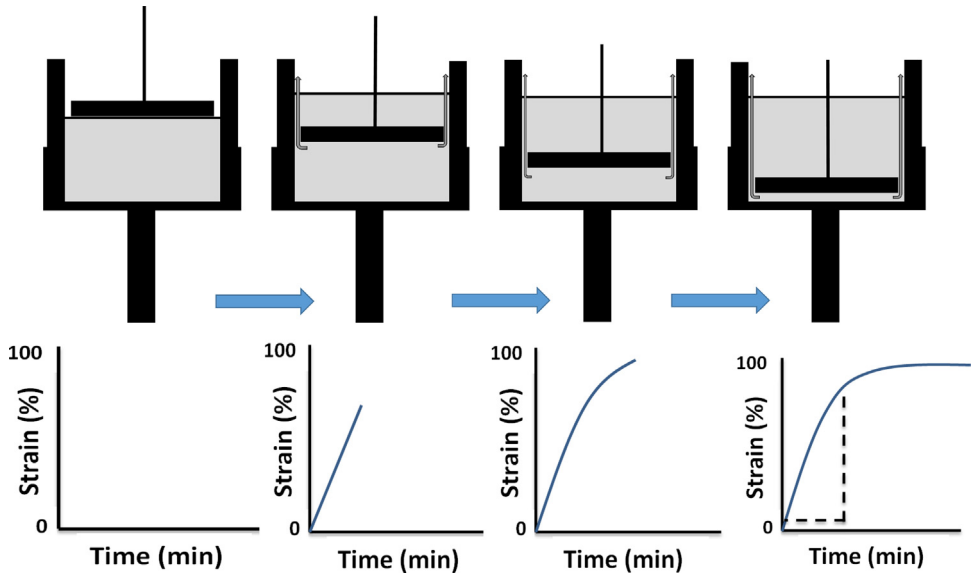

Fig. 6. Schematic of DMA methodology. The lid is equipped with a sensor that records the initial height of the sample. When the methodology is started the descending lid applies a sinusoidal force of 100 mN to the sample, causing the slurry to deform and move around the sides of the lid. Strain (slurry displacement) is recorded with time. A strain versus time plot is generated by the Pyris Manager software and the slope of the line before ultimate compression determines the slurry deformation rate.

more discontinuous compared to its fast flow counterpart which has a more homogenous, continuous structure, which may indicate greater mechanical strength. It should be noted that the cited literature plots [14], [15] depict axes with varying metrics. These citations are used to describe the method by which pressure-flow characterisation was carried out in this study. GE Healthcare data sheets depict similar profiles to the ones obtained in this study [25], [26]. Differences in critical velocity values reported in this study may be attributed to different packing techniques in the different columns used [27]. The pressure-flow profiles obtained by GE Healthcare use production scale columns (AxiChrom, BPG) and mainly pack-in-place and axial mechanical compression packing, whilst this study uses lab-scale XK16 columns under the flow packing technique. It is worth highlighting that the most critical aspect of this study is that the same batch of resins were used in the application of all techniques reported in this study.

3.2. Dynamic mechanical analysis (DMA)

This technique characterises mechanical properties based on the viscoelasticity of a small sample of resin. Conventional DMA is used to characterise homogeneously shaped biomaterials to determine elastic properties such as Young's modulus [17] however, we have adapted the technique such that it characterises the properties of a slurry. The equipment is composed mainly of a pan and a lid, equipped with sensors. The lid in particular is equipped with a sensor that allows it to stop just at the surface of the slurry once in descent. When the methodology is started, a sinusoidal force is applied at a constant frequency. As the lid descends, the slurry moves around the sides of the lid and this movement is recorded as a displacement percentage with time. Meanwhile, a time-strain profile is generated, where strain is the displacement of the lid through the resin bed recorded as a percentage. Once a strain threshold is exceeded, the rate of increase is vastly reduced or the plot begins to level out completely and at this point ultimate compression is reached. This is either when the lid has hit the bottom of the pan, or when little or no further deformation of the slurry can be achieved with constant force. For consistency, the slope of the line is taken before ultimate compression and this provides information about the movement of the lid through the slurry with constant force. A strain versus time plot is generated by the Pyris Manager software and the slope of the line before ultimate compression determines the slurry deformation rate. The slope of the line is manually fitted from the origin to the point before ultimate compression using the in-built slope function in the Pyris Manager software. The units are recorded as%/min (Fig. 6). The less viscous the media is, the quicker the lid will move through the slurry, therefore the higher the% strain per minute. The procedure is repeated 3 times for each resin (Fig. 7).

Fig. 8a shows the slurry deformation rates for each resin using the DMA technique. Capto Q has the slowest slurry deformation rate at 0.36%/min, followed by MabSelect – 0.55%/min, Q-Sepharose HP and Sepharose 6FF – 1.1%/min, Sepharose CL–6 B – 1.7%/min, Sepharose 4 FF – 2.5%/min and Sepharose CL–4 B – 3%/min.

Fig. 8b shows the graph obtained by plotting the reciprocal of the SDR values for each resin. The resulting parameter was termed 'slurry resistance ($1/\%min^{-1}$)'. This was done to more clearly show the trend between the pressure-flow technique and the DMA technique with particular focus on the gap between the more mechanically robust resins and the weaker resins. The results show Capto Q has the highest slurry resistance of 2.8, followed by MabSelect – 1.81, Q-HP and S6FF – 0.90, SCL6 B – 0.59, S4FF – 0.4 and SCL4 B – 0.3.

The same trends observed in Fig. 3 are observed in Fig. 8b. The results from Fig. 8b show that Capto Q is most resistant to deformation, followed by MabSelect, Q-Sepharose High Performance and Sepharose 6 Fast Flow, Sepharose CL-6B, Sepharose 4 Fast Flow and Sepharose CL-4B. Similar to the trends observed in section 3.1, the results also show that Q-Sepharose High Performance and Sepharose 6 Fast Flow exhibit very similar viscoelastic properties. Both resins contain 6% agarose however there are differences in their average bead sizes and pore sizes. Pore size is influenced by a number of factors, including the extent of cross linking which influences mechanical rigidity [1]. This becomes of relevance when the beads move past each other through the gaps as the lid descends and the gap size of 500 μm is large enough such that it does not allow for radial restriction/compression of single beads. The trade-off between the fact that Q-HP has a larger average pore size than S6FF, but S6FF has a larger bead size range, would mean that there are fewer S6FF beads for the same given volume. This could explain

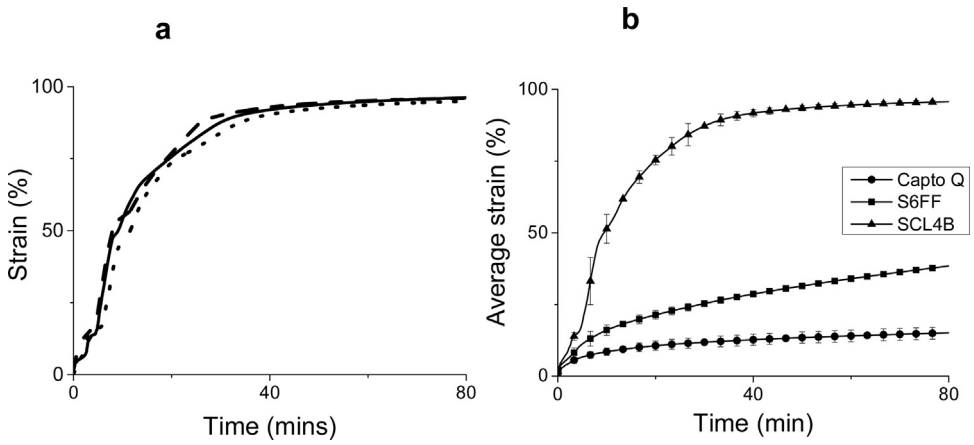

Fig. 7. (a) Strain v time plot for 3 repeats of Sepharose CL–4 B (4% cross-linked agarose) (one solid line, one dashed line, one dotted line). (b) Averages of 3 out of 7 resins – Capto Q (7% highly cross-linked agarose) (circles) – SDR 0.36%/min, Sepharose 6FF (6% cross-linked agarose) (squares) – SDR 1.1%/min and Sepharose CL–4 B (4% cross-linked agarose) (triangles) – SDR 3%/min. Error bars representing strain are standard deviations taken from the 3 repeats of each resin. An error bar is plotted once every 250 data points.

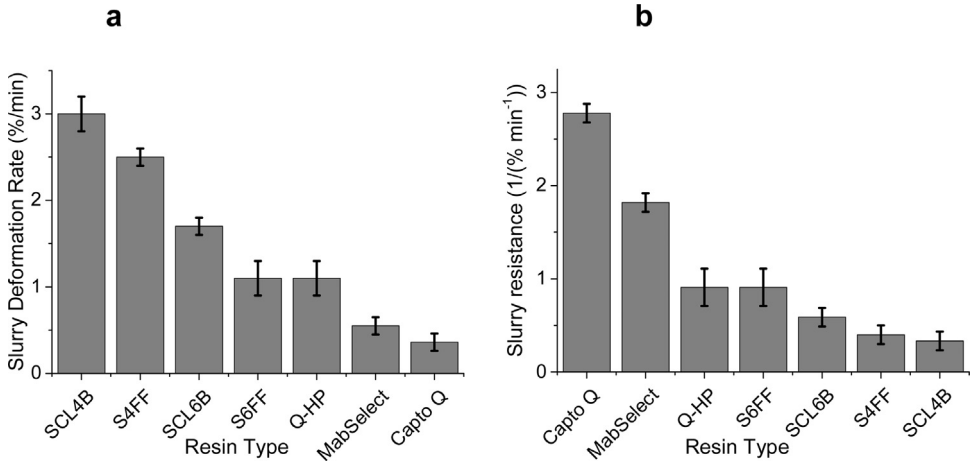

Fig. 8. (a) SDR for all 7 resins. For all resins, the slope of the lines for all three repeats are taken and averaged. The bar represents the average value and the error bars are standard deviations based on the three repeats. Capto Q has the slowest slurry deformation rate at 0.36%/min, followed by MabSelect – 0.55%/min, Q-Sepharose HP and Sepharose 6FF – 1.1%/min, Sepharose CL–6 B – 1.7%/min, Sepharose 4 FF – 2.5%/min and Sepharose CL–4 B – 3%/min. (b) Parity plot – Slurry resistance. The values are obtained by calculating 1/SDR values obtained for all 7 resins. This can then be better compared to Fig. 4. Capto Q has the highest slurry resistance of 2.8, followed by MabSelect – 1.81, Q-HP and S6FF – 0.90, SCL6 B – 0.59, S4FF – 0.4 and SCL4 B – 0.3.

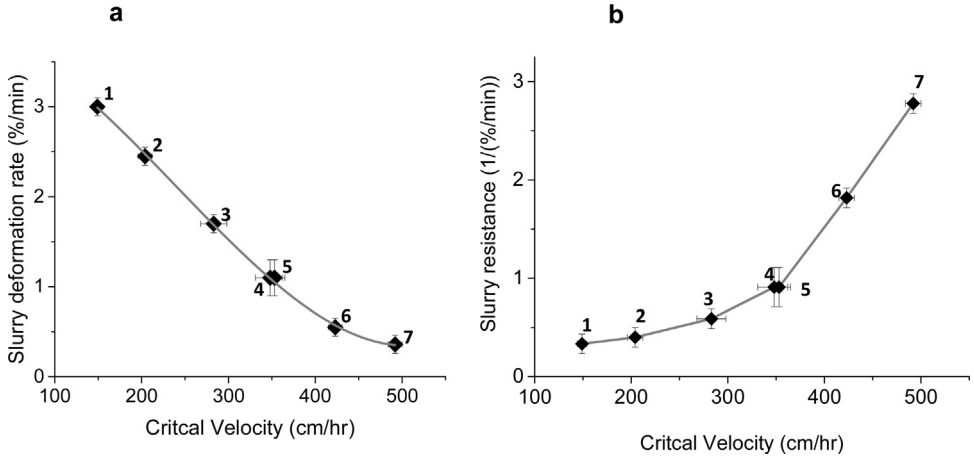

Fig. 9. (a) SDR values shown in Fig. 8(a) plotted against ucrit values shown in Fig. 4. Plot shows strong negative trend (b) Parity plot showing slurry resistance. Slurry resistance values are calculated as 1/SDR. Plot shows strong positive trend. 1- Sepharose CL-4B, 2- Sepharose 4 Fast Flow, 3 – Sepharose CL-6B, 4–Sephrose 6 Fast Flow, 5–Q-Sepharose High Performance 6–MabSelect, 7–Capto Q.

why the two resins have similar SDR values. The results also show the differences in viscoelastic properties between SCL6 B and S6FF, as well as SCL4 B and S4FF. Further explanations for the observed trends are outlined in Section 3.1. The data from Figs. 4 and 8 are plotted to establish a trend (Fig. 9).

3.3. Data correlation – pressure-flow vs dynamic mechanical analysis

Fig. 9a shows a strong negative correlation between critical velocity and slurry deformation rate for all 7 resins used in this study. This means that the stronger resins such as MabSelect and Capto Q have low SDRs and high u_{crit} values and the opposite is true for mechanically weaker resins such as SCL4 B and S4FF. The trend begins in a linear fashion with the first five resins but then tails off when the more mechanically robust resins appear. This representation of results indicates that as the resins become mechanically more similar and the difference in mechanical properties becomes less significant.

Fig. 9b shows a parity plot of Fig. 9a and the y-axis is represented as 'slurry resistance'. The values are calculated based on 1/SDR for each resin. The trend observed is a positive polynomial trend for slurry resistance against critical velocity. The first 5 resins show a gradual increase in mechanical resistance, however, the difference in mechanical strength becomes more apparent when the more robust resins (MabSelect and Capto Q) are plotted. This plot better demonstrates the disparity in mechanical behaviour between each resin and depicting the data in this way correlates positively with the pressure-flow data and is more easily comparable. Both plots show that DMA can be used as a combinatory technique to pressure-flow for the characterisation of chromatography media.

DMA has shown additional benefits in its use for resin characterisation. It allows for the use of small quantities of sample (~1 ml) and requires relatively little preparation. The low force of 100 mN applied in a sinusoidal manner is non-destructive to the media over an extended period of time (80 min). Given these advantages, it can potentially be used to investigate the mechanical properties of other media types, e.g. non-agarose based resins. It may also be used in the development of new resins for rapid testing post-emulsification.

4. Conclusion and potential applications

Currently, manufacturers use the pressure-flow characterisation technique to decipher mechanical limits of chromatography media by packing columns up to many litres in size. This is not only costly, but it is also time-consuming in its preparation and it requires a number of buffers to be used. We have developed a DMA technique that does not require the use of multiple buffers and uses a much reduced quantity of resin. The development of this technique considered a number of factors also associated with pressure-flow characterisation, including bead size, pore size and slurry concentration. This technique was tested on seven resins with varying mechanical properties and compared to their pressure-flow characteristics. The results show a strong correlation between both techniques. Using the pressure-flow method, the most robust resin (Capto Q) had a critical velocity 3.3 times higher than Sepharose CL-4B, whilst the DMA technique showed Capto Q to have a slurry deformation rate 8.3 times lower than Sepharose CL-4B. This could be due to increased sensitivity of mechanical changes as the sample volume used for DMA is much smaller than that of pressure-flow. This correlation indicates that DMA can be used as a combinatory technique for determining mechanical performance of a given resin. Although additional tests can always be performed to increase confidence in its application to other media types, the results from this study show definitive correlations between the two techniques for agarose-based resins. The correlation further suggests that DMA may be applied to predict pressure-flow characteristics. This technique may also be useful for rapid testing of a range of resins post-emulsification and during the development of new resins. Furthermore, it may also be used to test resins exposed to different conditions in the column as well as at different stages of its lifetime during bioprocessing. It may also be considered to investigate the impact of exposure to varying mechanical stresses during operation of large-scale chromatography.

Acknowledgments

This work was supported by theEPSRC, Eli Lilly & Co., UCL Eastman Dental Instituteand UCL Department of Biochemical Engineering. The support is gratefully acknowledged.

References

[1] N. Ioannidis, Manufacturing of Agarose-based Chromatographic Media with Controlled Pore and Particle Size, University of Birmingham, 2009.
[2] G. Jagschies, G. Sofer, L. Hagel, Handbook of Process Chromatography – Development, Manufacturing, Validation and Economics, 2nd ed., Elsevier, 2008.
[3] M. Andersson, Characterisation of Chromatography Media Aimed for Purification of Biomolecules, Uppsala Universitet, 2014.
[4] A. Jungbauer, Chromatographic media for bioseparation, J. Chromatogr. A 1065 (1) (2005) 3–12.
[5] A. Gerstein, Molecular Biology Problem Solver: A Laboratory Guide, 2nd ed., Wiley, 2004.
[6] Y. Mu, A. Lyddiatt, A.W. Pacek, Manufacture by water/oil emulsification of porous agarose beads: effect of processing conditions on mean particle size, size distribution and mechanical properties, Chem. Eng. Process. Process Intensif. 44 (10) (2005) 1157–1166.
[7] Q.-Z. Zhou, L.-Y. Wang, G.-H. Ma, Z.-G. Su, Multi-stage premix membrane emulsification for preparation of agarose microbeads with uniform size, J. Membr. Sci. 322 (1) (2008) 98–104.
[8] Q.-Z. Zhou, G.-H. Ma, Z.-G. Su, Effect of membrane parameters on the size and uniformity in preparing agarose beads by premix membrane emulsification, J. Membr. Sci. 326 (2) (2009) 694–700.
[9] Y. Yan, Z. Zhang, J.R. Stokes, Q.Z. Zhou, G.H. Ma, M.J. Adams, Mechanical characterization of agarose micro-particles with a narrow size distribution, Powder Technol. 192 (1) (2009) 122–130.
[10] N. Ioannidis, J. Bowen, A. Pacek, Z. Zhang, Manufacturing of agarose-based chromatographic adsorbents – effect of ionic strength and cooling conditions on particle structure and mechanical strength, J. Colloid Interface Sci. 367 (1) (2012) 153–160.
[11] K. Keller, T. Friedmann, A. Boxman, The bioseparation needs for tomorrow, Trends Biotechnol. 19 (11) (2001) 438–441.
[12] A. Ellis, J.C. Jacquier, Manufacture and characterisation of agarose microparticles, J. Food Eng. 90 (2) (2009) 141–145.
[13] P. Gavara, N. Bibi, M. Sanchez, M. Grasselli, M. Fernandez-Lahore, Chromatographic characterization and process performance of column-packed anion exchange fibrous adsorbents for high throughput and high capacity bioseparations, Processes 3 (1) (2015) 204–221.
[14] J.J. Stickel, A. Fotopoulos, Pressure-flow relationships for packed beds of compressible chromatography media at laboratory and production scale, Biotechnol. Progr. 17 (4) (2001) 744–751.
[15] R. Tran, J.R. Joseph, A. Sinclair, D. Bracewell, Y. Zhou, N.J. Titchener-Hooker, A framework for the prediction of scale-up when using compressible chromatographic packings, Biotechnol. Progr. 23 (2) (2007) 413–422.
[16] T. Warner, S. Nochumson, Rethinking the economics of pensions, BioPharm Int. 22 (3) (2003) 15–39.
[17] L. Moroni, J.R. De Wijn, C.A. Van Blitterswijk, 3D fiber-deposited scaffolds for tissue engineering: influence of pores geometry and architecture on dynamic mechanical properties, Biomaterials 27 (7) (2006) 974–985.
[18] T. Meyvis, B. Stubbe, A comparison between the use of dynamic mechanical analysis and oscillatory shear rheometry for the characterisation of hydrogels, Int. J. Pharm. 244 (2002) 163–168.
[19] M.C. Nweke, M. Turmaine, R.G. McCartney, D.G. Bracewell, Drying techniques for the visualisation of agarose-based chromatography media by scanning electron microscopy, Biotechnol. J. 12 (2016) 1600583.
[20] P. DePhillips, A. Lenhoff, Pore size distributions of cation-exchange adsorbents determined by inverse size-exclusion chromatography, J. Chromatogr. A 883 (2000) 39–54.
[21] C. Tarmann, A. Jungbauer, Adsorption of plasmid DNA on anion exchange chromatography media, J. Sep. Sci. 31 (14) (2008) 2605–2618.

[22] A.M. Hardin, C. Harinarayan, G. Malmquist, A. Axen, R. van Reis, Ion exchange chromatography of monoclonal antibodies: effect of resin ligand density on dymanic binding capacity, J. Chromatogr. A 20 (1216) (2009) 4366–4371.
[23] Q.-Z. Zhou, L.-Y. Wang, G.-H. Ma, Z.-G. Su, Preparation of uniform-sized agarose beads by microporous membrane emulsification technique, J. Colloid Interface Sci. 311 (1) (2007) 118–127.
[25] G.E. Healthcare, Packing MabSelect ™ and MabSelect SuRe ™ Media Using Verified Methods, GE Healthcare, Uppsala, Sweden, 2015, pp. 110.
[26] J. Avallin, A. Nilsson, M. Asplund, N. Pettersson, T. Searle, C. Jägersten, Columns Upto 1600 Mm in Diameter Packed with Protein A Chromatography Medium Using Axial Mechanical Compression, GE Healthcare, Uppsala, Sweden, 2016, pp. 291.
[27] M. Dorn, F. Eschbach, D. Hekmat, D. Weuster-Botz, Influence of different packing methods on the hydrodynamic stability of chromatography columns, J. Chromatogr. A (2017).
[28] L. Hagel, M. Ostberg, T. Andersson, Apparent pore size distributions of chromatography media, J. Chromatogr. A 743 (1) (1996) 33–42.
[29] M. Barrande, et al., Characterisation of porous materials for bioseparation, J. Chromatogr. A 1216 (41) (2009) 6906–6916.